

# Mars Observer Trajectory and Orbit Design

Joseph G. Beerer\* and Ralph B. Roncoli\*

*Jet Propulsion Laboratory, California Institute of Technology, Pasadena, California 91109*

The Mars Observer launch, interplanetary, Mars orbit insertion, and mapping orbit designs are described. The design objective is to enable a near-maximum spacecraft mass to be placed in orbit about Mars. This is accomplished by keeping spacecraft propellant requirements to a minimum, selecting a minimum acceptable launch period, equalizing the spacecraft velocity change requirement at the beginning and end of the launch period, and constraining the orbit insertion maneuvers to be coplanar. The mapping orbit design objective is to provide the opportunity for global observation of the planet by the science instruments while facilitating the spacecraft design. This is realized with a Sun-synchronous near-polar orbit whose ground-track pattern covers the planet at progressively finer resolution.

## Introduction

THE Mars Observer project is planning the United States' first visit to the Red Planet in more than a decade. The mission objective is to perform geological and climatological studies of the entire planet from a low, nearly circular mapping orbit. The launch is scheduled for September 1992 aboard a Titan III/ Transfer Orbit Stage (TOS) launch vehicle. A Type II heliocentric transfer with a deep space maneuver is planned. The spacecraft will approach Mars over the north pole and be maneuvered into an elliptical capture orbit with a descending node near 5 p.m. local mean solar time. Because a mapping orbit with a 2 p.m. node is preferred for scientific reasons, a three-month waiting period is necessary for a minimum velocity change  $\Delta V$  transfer to the mapping orbit.

A near-circular, near-polar mapping orbit was selected in order to minimize the altitude variation the instruments must accommodate and to permit observation of the entire planet. A Sun-synchronous orbit was chosen to provide nearly constant solar geometry for the science observations and to facilitate spacecraft design. The mapping orbit period of nearly 2 h provides an 88 rev/7 Martian day near-repeating ground-track pattern.

In the mapping phase, extending over one Mars year (687 Earth days), the spacecraft will support continuous science data collection, except for the solar conjunction period and maneuver periods. The data are recorded and played back the following day during a single Deep Space Network tracking pass. Near the end of the mapping phase, the spacecraft will provide a relay for data from instruments delivered to the Mars surface by Soviet spacecraft launched in the 1994 opportunity.

The interplanetary trajectory and mapping orbit designs take advantage of two separate propulsion systems on the spacecraft. A bipropellant system performs the trajectory correction maneuvers during cruise, the Mars orbit insertion (MOI) maneuver, and the transfer into the mapping orbit. A monopropellant hydrazine system is used for attitude control during maneuvers, reaction wheel momentum unloading, and orbit trim maneuvers in the mapping orbit. Besides being more adaptable to multiple-cycle operations, the hydrazine system offers a low-contamination environment for the science instruments. Since operation of the bipropellant system poses a

risk to the spacecraft while deployed in the mapping configuration, the preliminary launch period design is based on minimizing the bipropellant margin at the beginning and end of the launch period.

## Launch Scenario

The Mars Observer spacecraft will be launched with a Titan III/TOS launch vehicle from the Cape Canaveral Air Force Station in Florida. The Titan III is derived from the Air Force Titan 34 series of boosters and is built by Martin Marietta Commercial Titan. The Titan III is an integrated launch vehicle consisting of a two-stage liquid propellant core vehicle, two strap-on solid rocket motors, and a payload carrier. The TOS is an inertially guided, three-axis-stabilized, single-stage, solid propellant upper-stage vehicle. It utilizes the SRM-1 solid rocket motor built by the United Technology Corporation. The TOS is being developed by the Orbital Sciences Corporation with Martin-Marietta Civil Space and Communications as the prime contractor.

The mission requires near-maximum performance from the launch system. The current Titan III/TOS injected mass to Mars performance requirement is 2502 kg. The injected mass capability is anticipated to increase as a result of performance improvement and options currently being considered; however, this paper only addresses the present injected mass requirement. To provide this performance, the launch system will implement a variable launch azimuth strategy with an elliptical park orbit. Launch azimuth varies with the time of launch so that the departure asymptote is maintained in the launch trajectory plane as shown in Fig. 1. This enables the TOS injection burn to be a coplanar burn, thereby maximizing performance. The elliptical park orbit provides a performance benefit compared to a circular park orbit since the orbital velocity is higher at TOS ignition, which occurs near periapsis of the park orbit. In the current implementation, the park orbit insertion will occur at a constant radius, velocity, and flight-path angle. This strategy simplifies both the Titan and TOS guidance software. The performance benefit of the variable azimuth strategy, assuming a 30-min launch window, is about 60 kg of additional injected mass vs only about 6 kg for the variable park orbit insertion strategy.

For spacecraft design and propulsion system sizing, a baseline launch period was defined to be 20 days in duration. As the spacecraft mass and launch vehicle capability become better defined, it is expected that the actual launch period will increase to 24–28 days. On each day in the launch period, two launch opportunities occur. These are known as the first and second daily launch windows. The first daily window has been selected because it provides shorter park orbit coast times and therefore minimizes the power demands on the TOS and

Received Dec. 11, 1989; revision received June 5, 1991; accepted for publication June 6, 1991. Copyright © 1991 by the American Institute of Aeronautics and Astronautics, Inc. The U.S. Government has a royalty-free license to exercise all rights under the copyright claimed herein for Governmental purposes. All other rights are reserved by the copyright owner.

\*Member of Technical Staff, Mission Design Section.

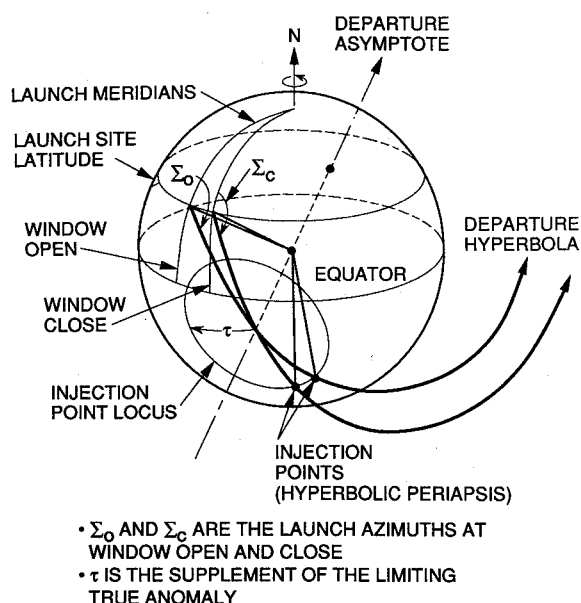


Fig. 1 Variable launch azimuth geometry.

spacecraft batteries. The minimum launch window duration has been defined to be 30 min to allow adequate launch operations flexibility. During the middle of the launch period, as performance permits, the launch windows will expand to up to approximately 2.5 h. Launch will occur between 10:30 a.m. and 3:00 p.m. Eastern Standard Time. Launch azimuths will be in the range of 93–112 deg to satisfy performance and range safety requirements.

The Titan booster will place the Mars Observer/TOS flight system in an approximate  $90 \times 200$ -nm park orbit. After coasting about 25 min, the 150-s TOS burn will inject the flight system onto the interplanetary trajectory. Fifteen minutes after TOS ignition, or approximately 12.5 min after TOS burnout, the spacecraft will separate from the upper stage and begin its deployment sequence. A few minutes after separation, the TOS performs a collision and contamination avoidance maneuver. The spacecraft will be acquired by the Deep Space Network's Canberra, Australia, tracking station within about 60 min after separation. The park orbit and escape hyperbola are illustrated in Fig. 2.

### Interplanetary Trajectory Design

The objective of the interplanetary trajectory design is to enable a near-maximum spacecraft dry mass to be delivered into the mapping orbit. Spacecraft dry mass is the spacecraft mass minus all propellant and pressurant masses. The selection of launch and arrival dates is based on the velocity changes necessary for interplanetary injection and Mars orbit capture and on the propulsive capabilities of the upper stage and spacecraft. There are no other mission requirements or constraints placed on the interplanetary trajectory design. For example, there are no Mars arrival date constraints. As a result, only two conditions must be met in order to determine the optimal set of launch and arrival dates. First, a launch period must be chosen that has the same interplanetary injection energy requirement, or  $C_3$  (defined as the square of the hyperbolic excess velocity), at the beginning and end of the launch period. By equalizing the  $C_3$  requirement at the ends of the period (which are the performance limiting dates), no injected mass capability is wasted. Second, following the same reasoning, the postinjection  $\Delta V$  requirement on the spacecraft must also be equalized at the beginning and end of the launch period. For the 1992 opportunity, Type II trajectories (heliocentric transfer angle  $> 180$  deg but  $< 360$  deg) with launch dates in September and October provide maximum spacecraft dry mass when applying these two conditions.

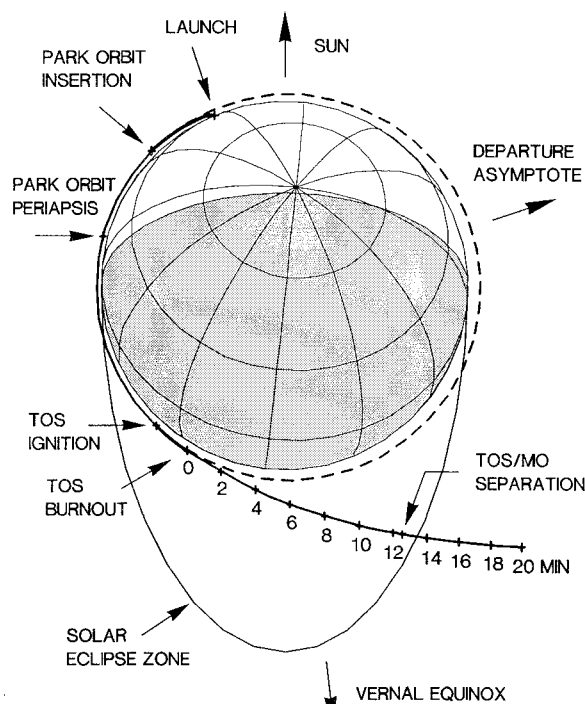


Fig. 2 Orbit normal view of launch trajectory.

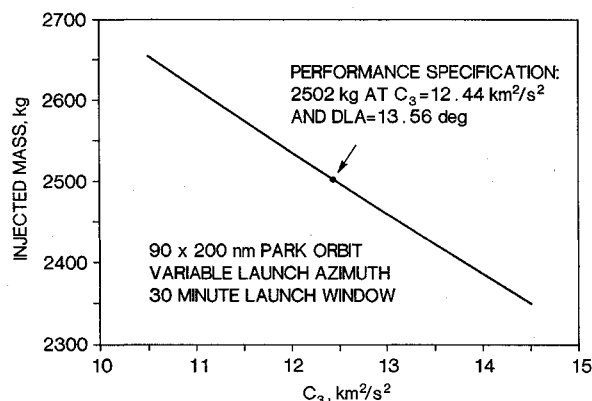


Fig. 3 TOS upper-stage injected mass performance.

Spacecraft dry mass capability is computed from the upper-stage injected mass performance, the spacecraft propellant mass and specific impulse, and the postinjection  $\Delta V$  requirement. The TOS injected mass performance is illustrated in Fig. 3. The total postinjection  $\Delta V$  requirement on the spacecraft is composed of the  $\Delta V$  necessary to execute midcourse corrections during the Earth to Mars interplanetary trajectory (80 m/s), to perform the Mars orbit insertion maneuver (launch day dependent), and to transfer the spacecraft into the mapping orbit (1367 m/s).

As a starting point, a design was determined consisting of ballistic trajectories that minimize the postinjection  $\Delta V$  requirements on the spacecraft. Ballistic is used here to define Earth-Mars transfer trajectories without any intermediate impulse. Figure 4 illustrates the required  $C_3$  for a ballistic 20-day launch period that extends from Sept. 18 to Oct. 8, 1992. The maximum spacecraft dry mass capability for this period is 1035 kg. The performance limiting trajectories occur on the first and last launch days. The same injection energy requirement,  $12.88 \text{ km}^2/\text{s}^2$ , is placed on the upper stage on both days satisfying the first condition stated earlier. Figure 5, however, indicates that the postinjection  $\Delta V$  requirement is much larger on the last launch day than on the first launch day. This means

that the last launch date defines the spacecraft propulsive requirement. It also means that the spacecraft propulsive capability is greatly underutilized at the beginning of the launch period.

Additional spacecraft dry mass capability was achieved by finding transfer trajectories that satisfy the second condition. At the beginning of the launch period, these trajectories are characterized by having a lower  $C_3$  and a higher postinjection  $\Delta V$  requirement. At the end of the launch period, the trajectories are similar to the ballistic minimum postinjection  $\Delta V$  transfers with only small differences in the injection energy and postinjection  $\Delta V$  requirements. A characteristic of the lower injection energy trajectories at the beginning of the launch period is that they require an additional impulse midway through the Earth to Mars transfer. Since this impulse causes a slight plane change, the maneuver is referred to as the broken plane maneuver (BPM).

Based on utilizing the Titan III/TOS (Ref. 1) and spacecraft performance capabilities, the near-optimal 20-day launch

period extends from Sept. 16 to Oct. 6, 1992. This permits a spacecraft dry mass of 1055 kg, 20 kg more than the ballistic launch period. This is due to both the lower injection energy requirements and lower postinjection  $\Delta V$  requirements. This launch period design has been designated the baseline. Figures 4 and 5 also illustrate the injection energy and postinjection  $\Delta V$  requirements for the ballistic and baseline 20-day launch period. This design requires a bipropellant loading of 1300 kg, whereas the tank capacity is 1364 kg. Figure 6 illustrates the spacecraft  $\Delta V$  and dry mass capability for the ballistic and baseline designs. (The maximum  $C_3$  value of  $12.44 \text{ km}^2/\text{s}^2$  for the period from Sept. 16 to Oct. 6, 1992, was chosen somewhat arbitrarily due to schedule constraints. However, subsequent analysis has shown insignificant mission benefit for other values of  $C_3$ .)

Table 1 gives the trajectory characteristics for the baseline design for selected days in the launch period. The data are for injections occurring at 0 h Greenwich Mean Time (GMT) on the given launch date. Actual injection times for launches in the first daily window are between 1600 and 2100 h GMT. (Note that the 20th launch date occurs on October 5 GMT.) The table gives the longitude difference between the Sun and the hyperbolic excess velocity  $V_\infty$  vector approaching Mars. This angle provides the approximate orbit orientation at ar-

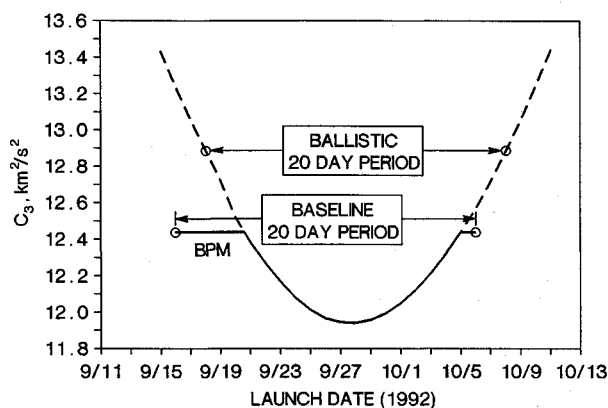


Fig. 4 Injection energy requirement over launch period.

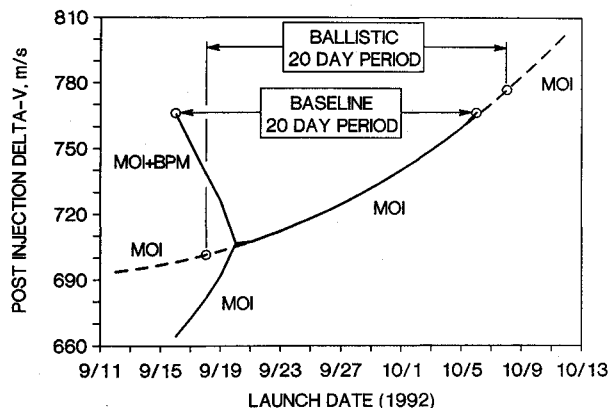


Fig. 5 Spacecraft velocity change requirement over launch period (trajectory dependent maneuvers only).

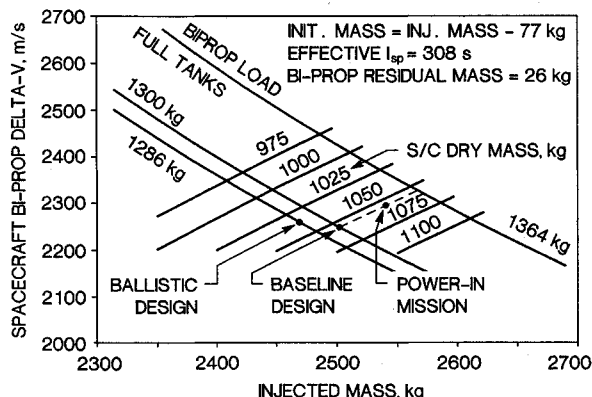


Fig. 6 Spacecraft  $\Delta V$  and spacecraft dry mass capability.

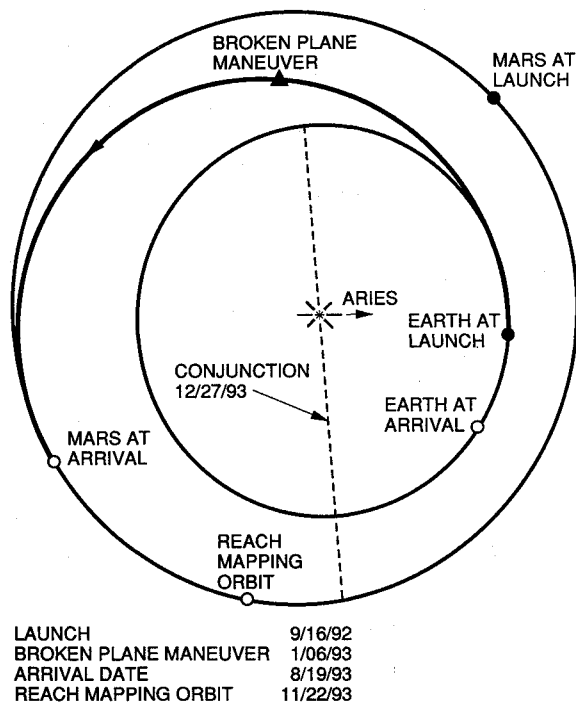


Fig. 7 Interplanetary trajectory for earliest launch date.

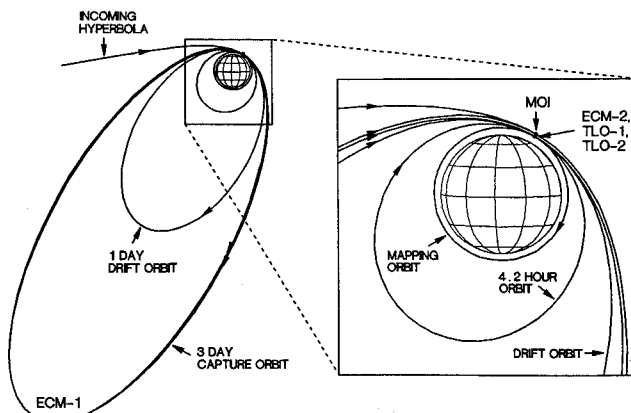


Fig. 8 Orbit transitions during orbit insertion phase.

Table 1 Trajectory characteristics for baseline 20-day launch period

| Launch date <sup>a</sup><br>1992 | Arrival date<br>1993 | $C_3$ ,<br>km <sup>2</sup> /s <sup>2</sup> | DLA, <sup>b</sup><br>deg | RLA, <sup>b</sup><br>deg | BPM <sup>c</sup><br>time,<br>launch date<br>+ days | BPM <sup>c</sup><br>$\Delta V$ ,<br>m/s | MOI <sup>c</sup><br>$\Delta V$ ,<br>m/s | Sun- $V_\infty$  <br>longitude<br>difference,<br>deg |
|----------------------------------|----------------------|--|--------------------------|--------------------------|--|---|---|--|
| 16 Sept.                         | 19 Aug.              | 12.44                                      | 13.2                     | 99.7                     | 112.4  | 101.1                                   | 664.5                                   | 85.2   |
| 17 Sept.                         | 20 Aug.              | 12.44                                      | 12.9                     | 99.8                     | 113.9  | 79.0                                    | 672.8                                   | 84.4   |
| 18 Sept.                         | 21 Aug.              | 12.44                                      | 12.7                     | 99.9                     | 115.5  | 57.0                                    | 681.7                                   | 83.5   |
| 19 Sept.                         | 22 Aug.              | 12.44                                      | 12.3                     | 100.0                    | 117.0  | 34.0                                    | 691.9                                   | 82.4   |
| 20 Sept.                         | 23 Aug.              | 12.44                                      | 11.8                     | 99.7                     | —  | —                                       | 706.6                                   | 81.4   |
| 21 Sept.                         | 20 Aug.              | 12.38                                      | 10.5                     | 98.5                     | —  | —                                       | 707.4                                   | 84.4   |
| 26 Sept.                         | 25 Aug.              | 11.97                                      | 10.8                     | 95.5                     | —  | —                                       | 721.2                                   | 81.8   |
| 6 Oct.                           | 6 Sept.              | 12.44                                      | 13.6                     | 89.8                     | —  | —                                       | 766.3                                   | 73.5   |

<sup>a</sup>Data are for interplanetary injection at 0 h GMT on the given launch date.

<sup>b</sup>Declination and right ascension of launch (departure) asymptote, DLA and RLA, respectively, in the Earth true equator and equinox of date coordinate system.

<sup>c</sup>BPM = broken plane maneuver.

<sup>d</sup>Mars orbit insertion  $\Delta V$  computed for capture orbit with  $r_p = 3950$  km and semimajor axis = 42,000 km.

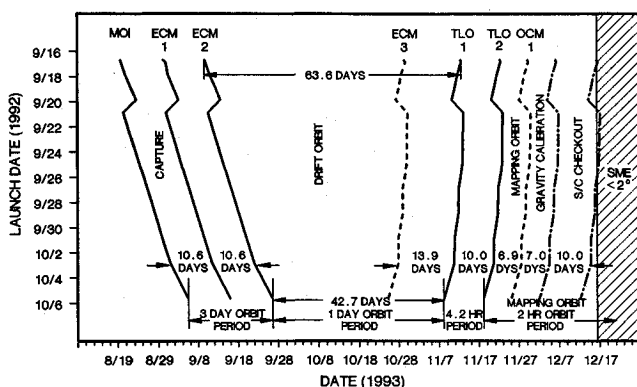


Fig. 9 Orbit insertion phase time line.

rival for a near-polar orbit. To achieve a 2 p.m. orbit orientation, this angle needs to be approximately 30 deg. Figure 7 shows the interplanetary trajectory for the opening launch day.

### Orbit Insertion Trajectory Design

The heliocentric transfer trajectories result in approach directions at Mars that differ from the direction of the Sun by angles of approximately 70–85 deg. With an approach over the Martian north pole and an in-plane orbit insertion maneuver, the resultant capture orbit has a descending node orientation of approximately 5:30–4:30 p.m. local mean solar time over the 20-day launch period. Since it is desired that the mapping orbit have a 2:00 p.m. descending node, a strategy involving seven maneuvers executed over about three months has been developed to achieve the desired node orientation, to meet mission constraints, to simplify the maneuver implementation, and to minimize the propellant expenditure. The transition from the interplanetary trajectory to the mapping orbit around Mars is called the orbit insertion phase. Figure 8 illustrates the orbits and identifies the deterministic maneuvers in this phase. In this figure, for descriptive purposes, the orbits are shown as coplanar. The timing of each of the maneuvers in the orbit insertion phase is illustrated in Fig. 9 as a function of launch date. The following paragraphs describe the purpose of each maneuver in this phase.

The MOI maneuver slows the spacecraft from the approach hyperbola into an elliptical orbit with a period of approximately three days. The target radius of periapsis of the capture orbit is 3950 km (altitude 553 km), and the target inclination is 92.9 deg (the inclination of the mapping orbit). The incoming hyperbola is biased high to account for delivery errors at MOI. Over the next two months, three ellipse change maneuvers (ECMs) are planned. The first two ECMs occur within three weeks of MOI. They will reduce the orbit periap-

sis and brake the spacecraft into the drift orbit, which has a period of approximately one day.

Although some science is performed in the drift orbit, it is primarily included in the design of the orbit insertion phase to minimize the propellant expended during the transition to the mapping orbit. Since rapid transition from the initial capture orbit to the desired 2:00 p.m. mapping orbit would require substantial out-of-plane  $\Delta V$ , an alternate approach was devised. The transition can be accomplished for a minimum  $\Delta V$  by using the drift orbit, which remains essentially inertially fixed. Therefore, the line of nodes drifts away from the Mars terminator at a rate of about 0.524 deg per day due to the orbital motion of Mars. The transition time using this approach, sometimes referred to as the natural drift mode, may take as long as three months depending on the launch date. The third ECM maneuver nominally requires zero  $\Delta V$  but is planned during the drift orbit to correct errors in the orbit, primarily inclination.

The next two maneuvers, designated TLO-1 and TLO-2 (transfer to low orbit), are large maneuvers that brake the spacecraft from the elliptical drift orbit into the near-circular mapping orbit. The timing of the maneuvers is such that the TLO-2 maneuver is executed when the descending node of an intermediate 4.2-h orbit reaches the desired 2:00 p.m. solar orientation. The transfer from the drift orbit to the mapping orbit is performed in two parts to reduce the inefficiency of the long burn time associated with a single large maneuver. The maneuvers are scheduled 10 days apart in order to allow the necessary time to plan and execute the second maneuver.

The final maneuver, OCM-1 (orbit change maneuver), is a trim maneuver planned to correct any errors in the mapping orbit. Once in the mapping orbit, the spacecraft will support a gravity calibration period of 7 sols [7 sols (Martian solar days) = 7.2 Earth days]. Continuous radiometric tracking data, excluding Earth occultations, will be obtained for the purpose of improving the knowledge of the Martian gravity field. During this period, the mapping orbit provides nearly uniform coverage of the planet with the ground-track spacing at the equator of about 240 km. The improved gravity field model is needed in order for the navigation team to provide the science teams with accurate orbit reconstruction and prediction information from the start of the mapping phase.<sup>1</sup> Following the gravity calibration period, the spacecraft will be deployed into the mapping configuration during a premapping spacecraft checkout period—not expected to exceed 10 days. The conclusion of this checkout period defines the end of the orbit insertion phase and occurs just before solar conjunction and a spacecraft command moratorium.

There are four maneuvers during the orbit insertion phase that will require many minutes of continuous thrusting (up to 28 min for the largest MOI burn) from two 490-N engines. The result of these long burns is that the orbit transfer will require more propellant than the impulsive calculations would in-

indicate since the entire  $\Delta V$  is not being applied at the optimum point of closest approach to Mars. This additional  $\Delta V$  is termed the gravity loss of the finite burn. The spacecraft will pitch at a constant rate about an inertially fixed axis during these burns. This strategy does not allow an optimal steering profile to minimize the gravity losses but is simpler to implement and can be designed to give results within a few meters per second of the optimal profile. Table 2 indicates the burn durations and gravity losses for the optimum constant pitch rate maneuvers. The total gravity loss allocation for the orbit insertion phase is 48 m/s. Figure 10 illustrates the geometry of the MOI finite burn for the earliest launch date. The thrust vector rotates 39 deg in the 24-min burn. The finite burn arc is just under 90 deg and is coplanar with the incoming hyperbola and the capture orbit.

**Table 2** Characteristics of orbit insertion maneuvers using constant pitch rate steering

| Launch date | Maneuver <sup>a</sup> | Total $\Delta V$ , m/s | Finite burn loss, m/s | Burn arc, deg | Burn duration, min |
|-------------|-----------------------|------------------------|-----------------------|---------------|--------------------|
| 16 Sept.    | MOI                   | 690.5                  | 20.8                  | 89.0          | 24.0               |
|             | ECM-2                 | 123.3                  | 0.1                   | 15.1          | 3.7                |
|             | TLO-1                 | 557.3                  | 6.2                   | 55.2          | 15.0               |
|             | TLO-2                 | 624.9                  | 10.9                  | 45.1          | 13.8               |
| 5 Oct.      | MOI                   | 792.9                  | 31.0                  | 99.8          | 27.9               |
|             | ECM-2                 | 123.3                  | 0.1                   | 15.0          | 3.7                |
|             | TLO-1                 | 557.2                  | 6.1                   | 54.8          | 14.9               |
|             | TLO-2                 | 625.0                  | 11.0                  | 44.9          | 13.7               |

<sup>a</sup>MOI = Mars orbit insertion; ECM = ellipse change maneuver; TLO = transfer to low orbit.

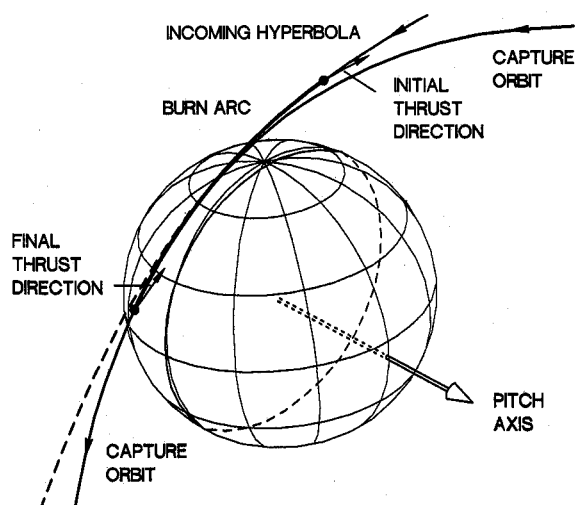


**Fig. 10** Mars orbit insertion finite burn.

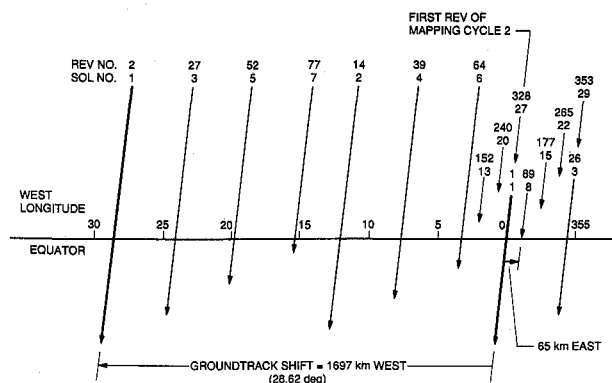


**Fig. 11** Ground-track pattern for exact 327/26 mapping cycle.

## Mapping Orbit Design

The mapping orbit design meets the science requirements for a low-altitude, near-circular, near-polar orbit which is Sun synchronous with the day-side equatorial crossing at 2 p.m. local mean solar time. The design also meets the science requirement for the orbit to have a repeating ground track of no more than 7 sols to allow fairly quick revisit times for observations in a given region. In addition, the design complies with the NASA planetary protection requirements.

A mapping orbit mean semimajor axis (SMA) of 3775.3 km was selected to provide a 7-sol near-repeating ground track. Selection of this SMA allows the gravity calibration to occur in the same orbit as the mapping orbit. Since most science instruments have small fields of view, it is desired that in the mapping phase the orbit revolutions build up a fine ground-track grid as the number of 7-sol cycles increase. The design of this grid dictates the precise SMA specification.

The ground-track repetition parameter  $Q$  represents the ratio of orbit revolutions to repeat period. For a Sun-synchronous orbit, the repeat period is measured in sols. The precise SMA was specified to give a  $Q$  of 6917/550, which is a variation of the 327/26 and 88/7 patterns. In the orbit producing the 88/7 pattern, rev 89 matches rev 1 exactly. A 1.1-km SMA decrease from this orbit causes rev 89 to fall 65 km east of rev 1, creating the 327/26 pattern, as shown in Fig. 11. From this orbit, a 0.1-km SMA increase causes rev 328 to fall 24.7 km west of rev 1, creating the 6917/550 pattern, as shown in Fig. 12. The 7-sol, 26-sol, and 550-sol periods are referred to as a repeat cycle, a mapping cycle, and a supercycle, respectively. Figure 12 shows that the ground track walks 58.6 km eastward after each repeat cycle. The instrument fields of view or footprints are shown in relation to this walk interval in Fig. 13.

Approximately 21 mapping cycles compose the supercycle. The supercycle will provide a nominal 3.1-km spacing between adjacent ground tracks at the equator. A characteristic of the selected supercycle is that the planet is sampled at progressively finer resolution throughout the mapping phase. Ideally, the supercycle would provide uniform coverage of the planet for instruments with smaller footprints. However, since the ground-track control in longitude, at the equator, is expected to be about  $\pm 20$  km, 99 percentile, the coverage may not be uniform.

Once the SMA is specified, the other orbit parameters can be selected to provide the desired orbital characteristics. The eccentricity and argument of periapsis are set to the values necessary for a frozen orbit. Frozen orbits are discussed in Ref. 2. A frozen orbit's shape and apsidal orientation remain nearly constant with time, thereby providing an almost constant altitude over a given latitude. The eccentricity needed to freeze an orbit is a function of the central body's gravity field. Since the Mars gravity field is not accurately known, the frozen eccentricity cannot yet be accurately determined. After the

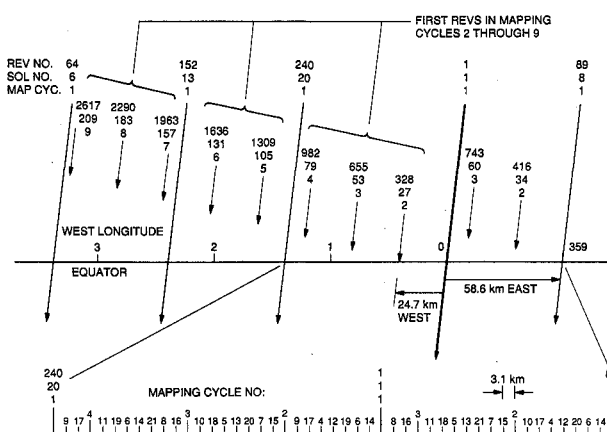


**Fig. 12** Ground-track pattern for 6917/550 supercycle.

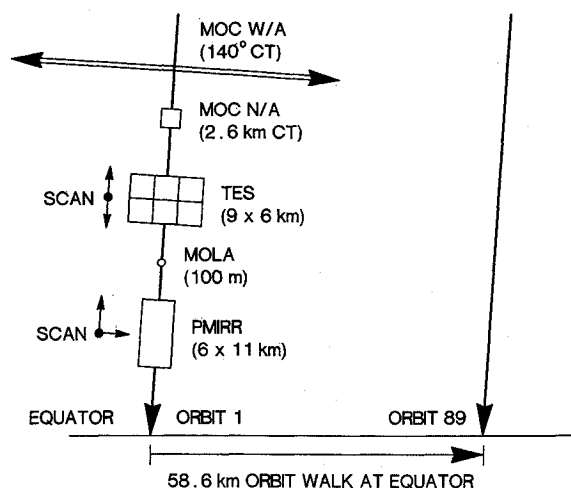


Fig. 13 Instrument footprints on Mars surface.

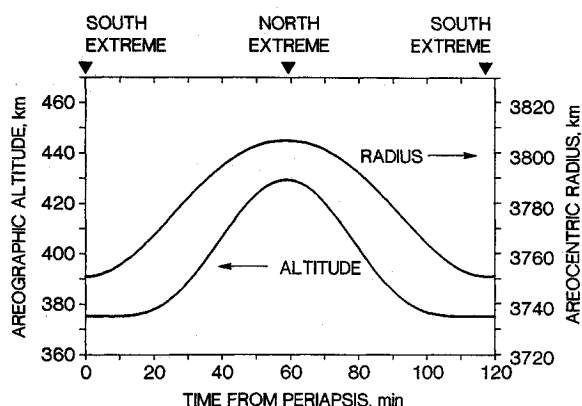


Fig. 14 Mapping orbit altitude and radius variation.

mapping orbit is established and the gravity field is more accurately defined, the frozen eccentricity will be computed and a maneuver performed to adjust the orbit to that value. The current estimate of frozen mean orbital eccentricity is  $0.007 \pm .006$  (3  $\sigma$ ). Figure 14 shows variations in the spacecraft areographic altitude and areocentric radius during one orbit revolution, based on a mean eccentricity of 0.007. Areographic altitude is approximately the height of the spacecraft above the Mars surface. It is measured relative to the United States Geological Survey mapping spheroid, which has an equatorial radius of 3393.4 km and a polar radius of 3375.7 km.

The orbit inclination is determined by the requirement for the orbit to be Sun synchronous. This requirement says that the orbit line of nodes shall maintain a constant angle with respect to the fictitious mean sun (FMS). The FMS moves eastward in the Mars equator plane at a rate equal to the mean orbital rate of Mars about the Sun. The FMS and the true Sun differ in position due to the obliquity and eccentricity of the Mars orbit. The effect of Mars' oblateness causes the orbit to precess. The amount of precession depends on inclination and SMA. Since SMA has already been determined to satisfy the ground-track requirements, only inclination can be selected to satisfy the Sun-synchronous requirement. For the orbit to precess eastward, the inclination must be between 90 and 180 deg. At 92.87 deg, the orbit precesses at the required rate of 0.524 deg per day.

Although the mapping orbit is Sun synchronous, the spacecraft experiences some variation in solar geometry since the difference in right ascension between the FMS and the true Sun can be as large as 13 deg. The angle that the Mars-Sun line makes with respect to the orbit plane varies from 16 to 40 deg. During its 118-min orbit period, the spacecraft will be in dark-

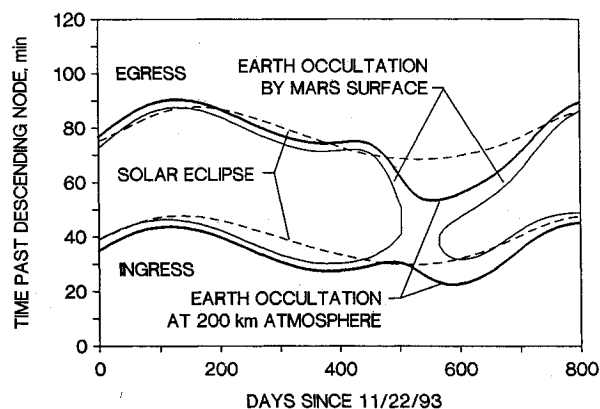


Fig. 15 Time of spacecraft in eclipse and occultation.

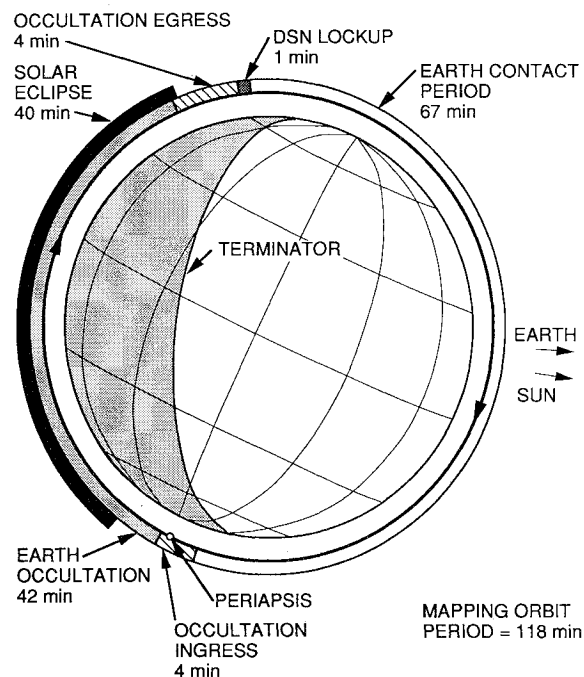


Fig. 16 Typical mapping orbit spacecraft events.

Table 3 Mapping orbit elements

|  | Mean   | Osculating at periapsis |
|--|--------|-------------------------|
| Semimajor axis, km                       | 3775.3 | 3766.2                  |
| Eccentricity                             | 0.0070 | 0.0038                  |
| Inclination <sup>a</sup> , deg           | 92.87  | 92.87                   |
| Ascending node <sup>a</sup> , deg        | 31.32  | 31.32                   |
| Argument of periapsis <sup>a</sup> , deg | -90.0  | -90.0                   |
| Mean anomaly, deg                        | 0.0    | 0.0                     |
| Periapsis radius, km                     | 3748.9 | 3751.1                  |
| Apoapsis radius, km                      | 3801.7 |                         |
| Nodal period, s                          | 7058.9 |                         |

<sup>a</sup>Mars equator and equinox of date coordinate system.

ness between 36 and 41 min. Figure 15 shows the solar eclipse ingress and egress times in the orbit as a function of time in the mission. This figure also shows Earth occultation event times. The period in each orbit when the spacecraft cannot see the Earth varies from 0 to 42 min. An orbit normal view of a typical mapping orbit with eclipse and occultation periods noted is shown in Fig. 16. Table 3 gives the mean orbital elements and the osculating elements at periapsis on the date of the maneuver into the mapping orbit, Nov. 22, 1993.

The mapping orbit design satisfies the NASA Planetary Protection orbital lifetime requirements without an end-of-

mission orbit raise maneuver. In accordance with international agreements not to contaminate Mars with terrestrial organisms during the initial period of biological exploration of the planet, the requirements state that the probability of accidental impact of the spacecraft (or any separated part of it) on Mars before Jan. 1, 2009, must be  $< 0.0001$ . Also, the requirements state that the probability of impact of the spacecraft on Mars between Jan. 1, 2009, and Jan. 1, 2039, be  $< 0.05$ . A mapping orbit with an SMA of 3767.2 km or higher will satisfy these requirements.

### Power-In Option

An undesirable characteristic of the present mission design is the long time between arrival at Mars and entry into the mapping orbit. As a result of this extended orbit insertion period, mapping operations are commenced just before solar conjunction and the Mars dust storm period. Since mapping operations will cease for several weeks around solar conjunction, and since a number of science instruments require a clear atmosphere to see the Mars surface, there is a strong desire to reach the mapping orbit earlier. Therefore, the project is carrying an option, known as the power-in option, which can shorten the time in the drift orbit by several weeks. Power-in is accomplished by incorporating a slight plane change into the MOI maneuver and by adding an out-of-plane component to ECM-1 that occurs near apoapsis of the capture orbit to move the orbit node toward 2 p.m. For this option, the capture orbit inclination requires a bias away from the mapping orbit inclination because the apoapsis maneuver will change the inclination as well as the node.

For the three-day capture orbit design, about 1.5 kg of propellant is needed for each day of drift time reduction. The propellant expenditure is less if the maneuver was performed in a larger orbit. However, orbits with periods greater than three days provide less operations flexibility and have unacceptably large uncertainties (greater than one day) in their periods due

to navigational errors. Operations planning is simplified if these uncertainties are kept to less than one day.

Because of current mass constraints, there is no propellant budgeted for power-in. However, a good TOS injection, which reduces propellant needed for midcourse corrections, or a launch in the middle of the launch period (postinjection  $\Delta V$  is less) will provide excess propellant. Also, should the launch vehicle performance capability exceed the present requirement, additional bipropellant could be loaded for power-in, although this performance improvement could be used to extend the launch period or to extend the mapping mission by loading additional hydrazine. A decision on power-in will be made during the cruise to Mars.

### Conclusions

Trajectories have been found that nearly maximize the spacecraft dry mass at Mars for the 1992 Mars Observer mission. A characteristic of these trajectories is that several months in Mars orbit are required before reaching the mapping orbit. A mapping orbit design has been completed that facilitates the spacecraft and instrument design and satisfies the science requirements. An option exists for accelerating the transfer to the mapping orbit.

### Acknowledgments

This research was conducted by the Jet Propulsion Laboratory, California Institute of Technology, under contract with NASA. The authors wish to acknowledge, in particular, the mission design contributions provided by W. H. Blume, G. M. Horvat, and C. L. Yen.

### References

- <sup>1</sup>Esposito, P. B., and Demcak, S. N., "Mars Observer Orbital Accuracy Analysis: II," American Astronomical Society, Washington, DC, Paper 87-504, Aug. 1987.
- <sup>2</sup>Uphoff, C., "Orbit Selection for a Mars Geoscience/Climatology Orbiter," AIAA Paper 84-0318, Jan. 1984.